Genetic dissection of spermatogenic arrest through exome analysis: clinical implications for the management of azoospermic men

SUPPLEMENTARY MATERIAL AND METHODS

Replication cohorts:

The current study utilized the following two study populations to perform a targeted lookup of predicted as pathogenic variants in *ADAD2*, *TERB1*, *SHOC1*, *MSH4* and *RAD21L1* genes.

MERGE study cohort

The Male Reproductive Genomics (MERGE) study comprises mostly patients who present to the Centre of Reproductive Medicine and Andrology, Münster, Germany, for couple infertility. Those undergoing exome sequencing were selected predominantly for unexplained non-obstructive azoospermia. The full andrological workup did not provide a causal diagnosis and all were screened for chromosomal aberrations and Y-chromosomal AZF-deletions, which turned out normal. In total, the exome sequencing data of 652 men with lacking or severe, quantitatively impaired spermatogenesis was available of whom 57 had complete, bilateral meiotic arrest and negative TESE outcome.

GEMINI consortium

The Genetics of Male Infertility Initiative (GEMINI) is a NIH-funded effort to with the goal of identifying novel genetic causes of male infertility (https://gemini.conradlab.org/). The consortium is comprised of eighteen andrology/urology centers in eight countries and has a current focus on exome

sequencing in non-obstructive azoospermia cases. In total the exome sequencing data was available for 73 MA patients.

Informed consent and ethics approval

All patients (and family members where applicable) provided written informed consent to be included in the analyses and specifically exome sequencing. The study protocol was approved by the local ethics committees (Fundacio Puigvert: 2014/04c, Münster: 2010-578-f-S, GEMINI: 201502059).

Variant filtering and gene prioritization in the initial cohort

A standard variant filtering was applied to all samples as described in Riera-Escamilla et al. 2019[1]. Briefly, we selected missense variants, stop-gains/losses, and frameshift insertions/deletions, and filtered out common polymorphisms (≥5% in the general population) based on frequencies observed in dbSNP 138, the 1000G (http://www.1000genomes.org) and the genome aggregation database gnomAD (http://gnomad-old.broadinstitute.org/). Data were further filtered according to their potentially damaging effect depending on the type of variant. For single nucleotide variations, the prediction of pathogenicity was based on a series of prediction tools, including SIFT, Polyphen2_HDIV, Polyphen2_HVAR, Mutation Taster, and Mutation Assessor. An in-house index of pathogenicity (IP) was created as a score calculated on the basis of the five prediction tools employed, each providing a value ranging from 0 (null probability of being a deleterious variant) to 1 (full probability of being a deleterious variant). Not all prediction tools were always available; therefore, a ratio was calculated between the summary score of pathogenicity and the number of prediction tools available for a given variant. Hence, we established an arbitrary threshold of $IP > 0.6$, which means that the majority (not necessary all) of the

interrogated tools gave a 'pathogenic' score (see Table S8). We also considered as 'possibly pathogenic' all low-frequency frameshift variants and indels within non-repeated regions. Pathogenicity of the prioritized variants was also manually checked using Varsome (https://varsome.com/). Subsequently, the Integrative Genomics Viewer was employed to exclude possible false positive calls, and, finally, the prioritized variants were validated by Sanger sequencing or SYBRGreen based qPCR or +/- PCR (see primers in Table S9). Prioritization of genes was performed according to their putative role in spermatogenesis (testis expression, PubMed, model organisms).

Phasing of *STAG3* and *SHOC1* variants

A long-range PCR was performed to produce an amplicon including both *STAG3 and SHOC1* sequence variants, respectively (for primers see Table S9). The amplicons of correct sizes (~20 kb) were isolated from an agarose gel using the Monarch Gel Extraction Kit (New England Biolabs GmbH, Frankfurt, Germany). The purified products were used as templates for the library preparation of an Oxford Nanopore MinION (Oxford Nanopore Technologies, Oxford Science Park, UK) long-range sequencing runs. The sequencing library were prepared following the manufacturer´s instructions for the Ligation Sequencing Kit (SQK-LSK 109) and Native Barcoding Expansion Kit (EXP-NBD104, Oxford Nanopore Technologies). Sequencing was performed on a MinION flow cell (FLO-MIN106, Oxford Nanopore Technologies). A total number of 42.000 reads were sequenced yielding 329 megabases in total and an average coverage of 14.000 reads for the target region. Basecalling and Demultiplexing was performed using Guppy v3.2.6 implemented in the MinKNOW operating software from Oxford Nanopore. Reads were aligned against GRCh37.75 using Minimap2 v2.14. Only reads with the appropriate length of >19 kb were selected for subsequent variant

calling. Medaka v0.11.0 from Oxford Nanopore was used for variant calling and phasing.

Hematoxylin and Eosin staining

Testis biopsies were sectioned (section thickness 6µm), placed on dH_2O droplets on adhesive KP slides (Klinipath #PR-S-001) and stretched on a heating plate at 39˚C. After stretching, the slides were dried at RT overnight. The next day, the slides were placed in an oven for 1 hour at 60˚C to melt the paraffin. Slides were then deparaffinized and rehydrated as follows: 2 x 10 minutes xylene, 2 x 5 minutes absolute EtOH, 1x 2 minutes 90% EtOH, 1 x 70% EtOH and then washed in dH_2O. Tissue sections were then stained with Hematoxylin for 8 minutes and washed in running tap water for 10 minutes. Slides were subsequently rinsed in dH_2O followed by 10 dips in 95% EtOH. Following the wash step, tissue sections were counterstained with eosin for 1 minute and dehydrated through 1x 5 minutes 95% EtOH and 2x 5 minutes absolute EtOH. Finally, the slides were cleared in 2x 5 minutes xylene and mounted with Pertex® mounting medium (Histolab #00801).

Quantitative RT-PCR (qRT-PCR) analysis

qRT-PCR analysis of ADAD2 expression was performed in testicular tissues displaying different types of adult testis histology. RNA extraction was performed using a combination of two commercially available kits, the TRI Reagent (Sigma-Aldrich, St. Louis, MO, USA) and the AllPrep DNA/RNA kit (Sigma-Aldrich, St. Louis, MO, USA), according to the manufacturer's instructions. cDNA synthesis was carried out with the High-Capacity cDNA Reverse Transcription Kit (Life Technologies). qRT-PCR was performed using the TaqMan® Universal PCR Master Mix (Life Technologies) with the following standard thermal cycler conditions: 40 cycles at 95°C

for 30 s and 60°C for 1 min. We characterized one sample with Sertoli Cell Only (SCOS), two samples with spermatogonial arrest (including biopsy from the *ADAD2* variant carrier), two samples with spermatocytic arrest, and two samples with obstructive azoospermia (normal spermatogenesis based on histological examination). Molecular characterization was performed in whole tissue RNA-extracts, by expression analysis of four genes specific to different stages of spermatogenesis: *DAZ* (spermatogonia/early spermatocytes), *CDY1* (spermatids), *BRDT* (pachytene SPCs/round and elongating spermatids), and *PRM2* (spermatids/mature spermatozoa). *GAPDH* was used as the housekeeping reference gene. The employed commercial assays are detailed in Table S10. qRT-PCR runs were performed on a StepOne™ System (Applied Biosystems). All experiments were performed in triplicate.

Antibodies and fluorescent immunohistochemistry

Fluorescent staining was performed as previous described[2]. The following antibodies were used: mouse monoclonal against γH2AX (1:1000, Millipore #05-636, to detect meiotic DSBs and the XY body in pachytene nuclei, and apoptotic metaphases in case of pan-chromosomal signal), mouse monoclonal against acrosin (1:40, Biosonda, Chile #AMC-ACRO-C5F10-AS, to detect the acrosome in spermatids), and a rabbit polyclonal against H3Ser10ph (1:1000, Millipore #06-570, to detect metaphases). Primary antibodies were labeled with the appropriate secondary antibodies raised in goat conjugated with Alexa fluor 488 or 546 (both 1:500, Invitrogen #A-11001 or #A-11010).

Quantitative and qualitative analysis of immunofluorescent immunostainings of human testis biopsy sections and fluorescent imaging

The quantitative and qualitative analyses of the human testis biopsies were performed as previously described[2]. Additionally, the analysis was performed in a blinded fashion, meaning that the genetic variant that corresponded to the testis biopsy was unknown to the researcher performing the analysis. Fluorescent images were taken using a Zeiss LSM-700 confocal microscope with a 63x oil immersion Plan-Apochromat objective with ZEN2 software. Z-stack images were made with a 3.5x zoom. Image processing was performed using FIJI (version 1.52n). Thresholds for normal values were as described[2]; >43.9% tubules with early meiotic prophase cells, >82.6% of tubules containing XY body-positive nuclei, >7.74 XY bodies per XY body-positive tubule, >2.53 metaphases/mm^2, <11.5% apoptotic metaphases.

Statistical analysis

Data from 125,748 exomes available in gnomAD v2.1.1 database were used for the comparison of the frequency distribution of subjects with homozygous Loss of Function variants between cases (NOA patients) and controls (subjects in gnomAD v2.1.1_exomes). Frequencies were compared by Fisher's exact test.

In addition, we calculated the PopScore for each variant by using the Population Sampling Probability pipeline (PSAP)[3]. Briefly, PSAP models the significance of observing a single subject's genotype in comparison to genotype frequencies in unaffected populations (commonly referred to as the 'n-of-one' problem).

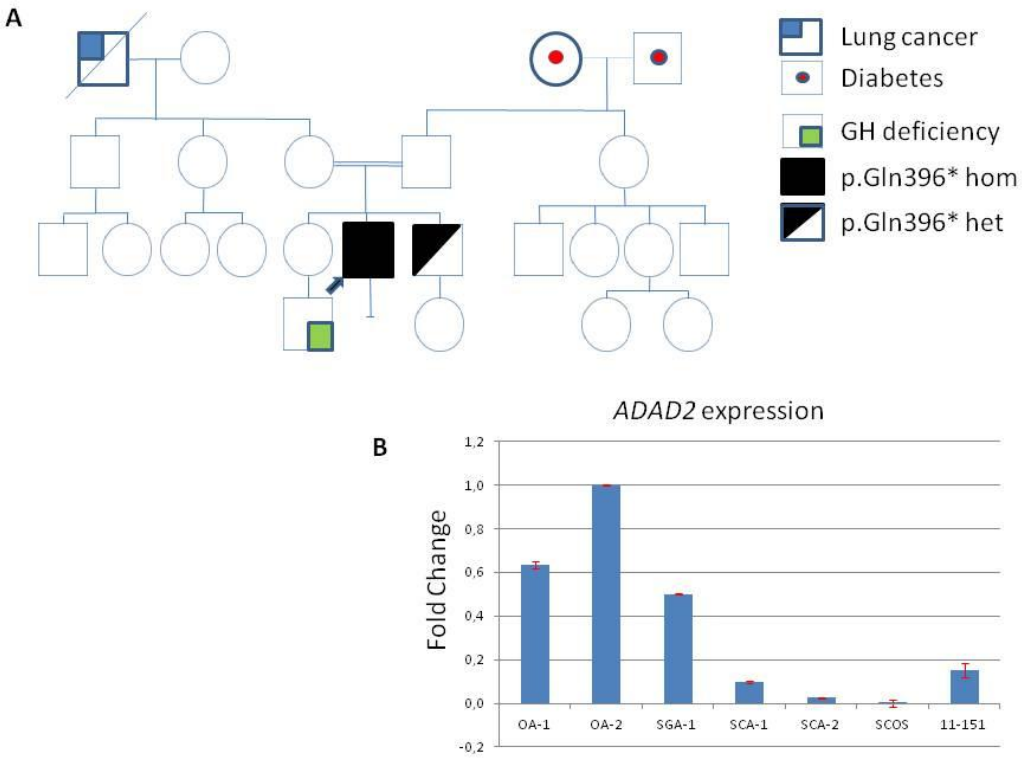

Figure S1. Investigation of patient 11-151, carrier of the *ADAD2* variant. A) The pedigree shows the segregation of the NM_139174.3:c.1186C>T variant. The lower-left arrow indicates the proband 11-151 who was subjected to WES analysis whereas his fertile brother's DNA was sequenced by Sanger sequencing. **B)** Expression evaluation of the *ADAD2* gene: Quantitative RT-PCR (qRT-PCR) analysis was performed to evaluate ADAD2 expression in biopsy samples of different types of adult testis histologies: i) one SCOS (Sertoli Cell-Only Syndrome); ii) one SGA: maturation arrest at the spermatogonial level; iii) the testis biopsy of the *ADAD2* variant carrier, also affected by SGA (11-151); iv) two SCA: maturation arrest at the spermatocytic level. Two samples with obstructive azoospermia (OA) were used as internal controls. Testis-derived RNA samples were first characterized for expression of four spermatogenic markers expressed at different stages of spermatogenesis: PRM2 (spermatids/mature spermatozoa); CDY1 (spermatids); BRDT (pachytene spermatocytes/round and elongating spermatids) and DAZ (spermatogonia/early spermatocytes). The analysis revealed germ-cell specific expression in the testis and a higher expression in spermatogonial arrest compared to spermatocytic arrest. The variant carrier displayed approximately 2.7-fold lower expression than the testis biopsies with SGA and wild type *ADAD2*.

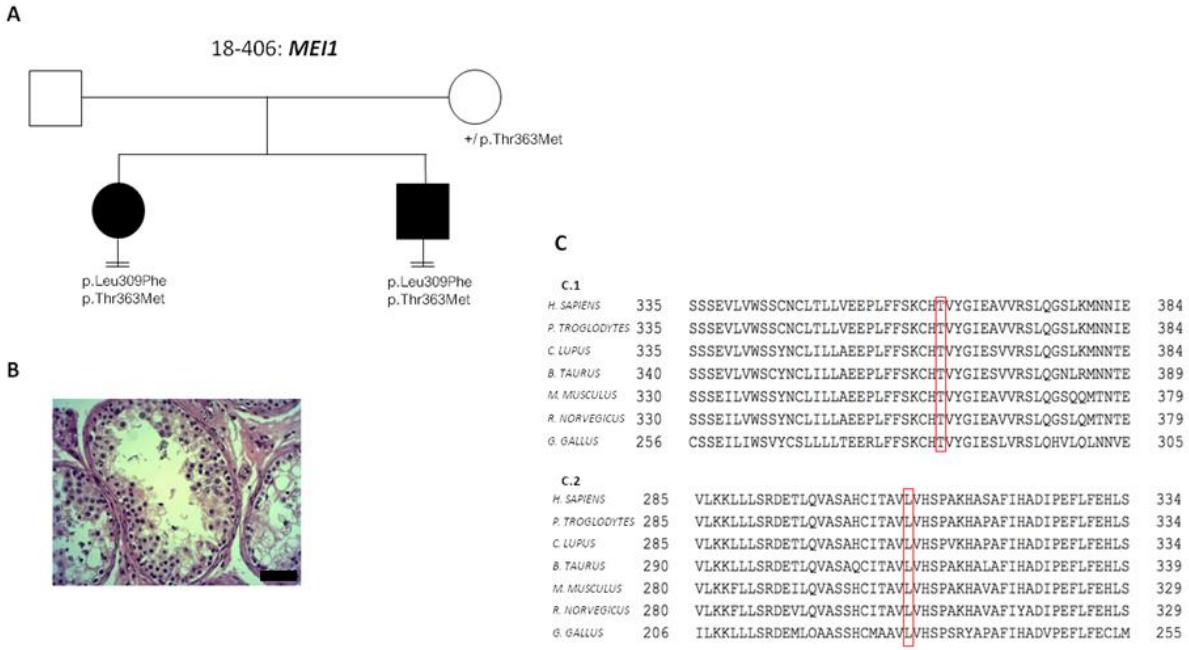

Figure S2. Investigation of patient 18-406, carrier of the *MEI1* variants. A) The pedigree shows the segregation of the NM_152513.4:c.925C>T;p.Leu309Phe and the NM_152513.4:c.1088C>T; p.Thr363Met variants. **B)** H&E staining of histological section from the testis biopsy of the patient carrying the MEI1 variant. Scale bar represents 50µm. **C)** Sequence alignment of MEI1 protein orthologs, performed by HomoloGene. Red box highlights the Leucine 309 and the Threonine 363 which are highly conserved among species.

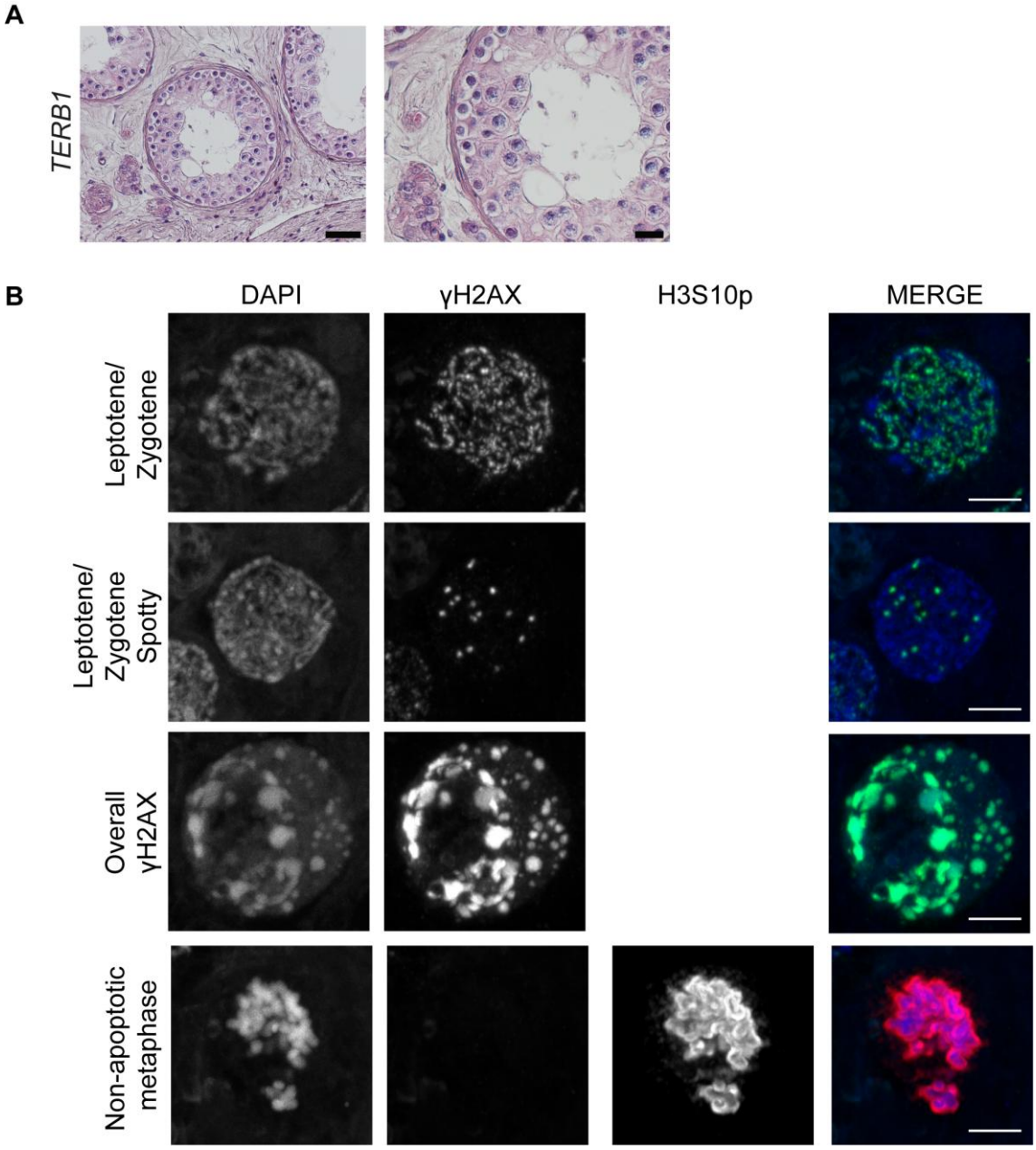

Figure S3. Meiotic progression analysis in patient 10-200 carrying the *TERB1* variant. A) H&E staining of histological sections from the testis biopsy of the patient carrying the *TERB1* variant. Scale bar on the left represents 50 µm and on the right, 20 µm. **B)** Immunofluorescent staining of histological sections from the testis biopsy of the patient carrying the *TERB1* variant using γH2AX (Green), H3S10p (red), and DAPI (blue). Scale bar represents 5µm. Early meiotic cells (leptotene/zygotene) were identified based on the presence of many γH2AX-positive patches. An aberrant more spotty γH2AX pattern was also observed in some nuclei, but no pachytene nuclei containing XY bodies could be identified. Instead many spermatocyte nuclei displayed intense γH2AX signal covering the DAPI (DNA) signal, indicating apoptosis. Few, non-apoptotic mitotic metaphases were observed.

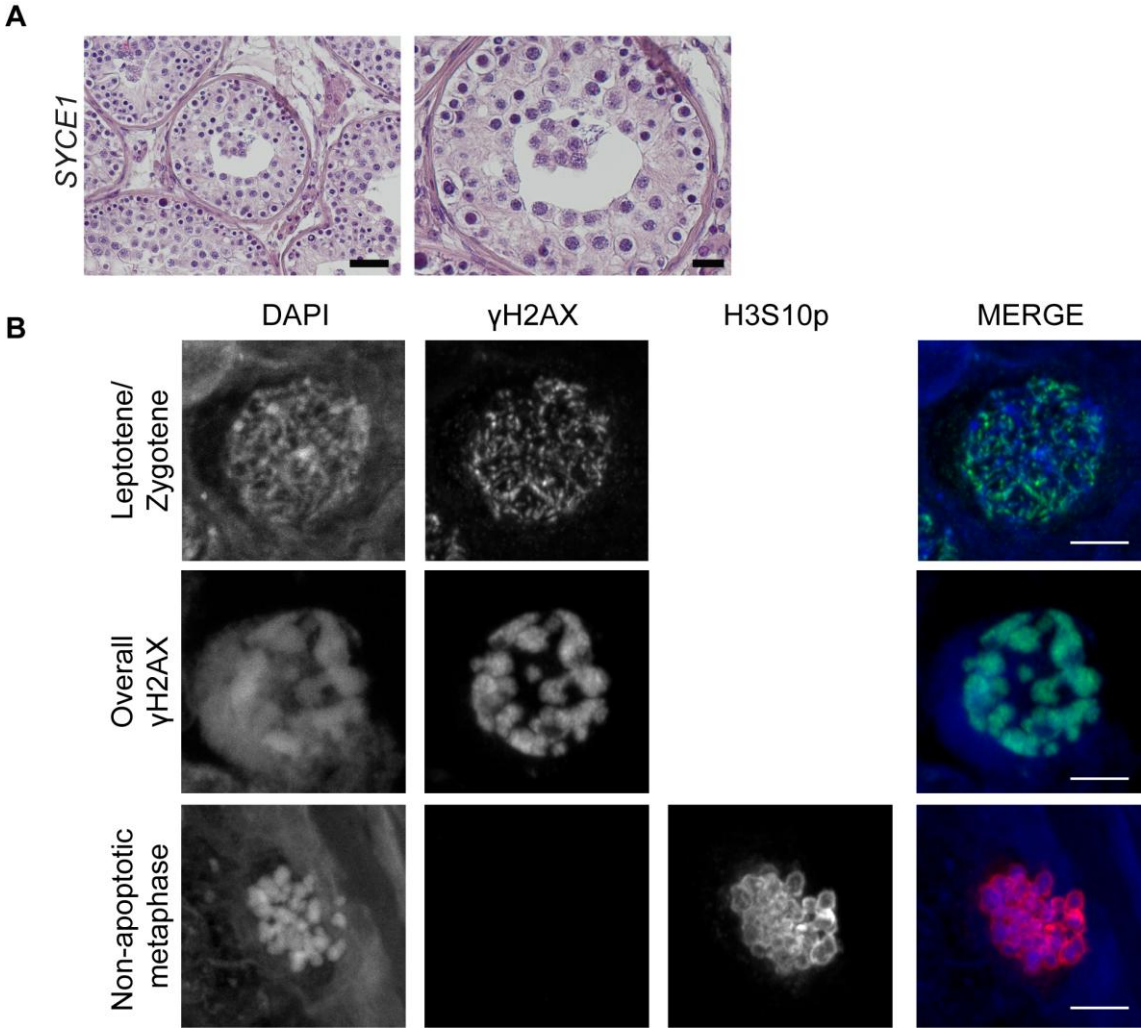

Figure S4. Meiotic progression analysis in patient 15-285 carrying the *SYCE1* variant. A) H&E staining of histological sections from the testis biopsy of the patient carrying the *SYCE1* variant. Scale bar on the left represents 50 µm and on the right, 20 µm. **B)** Immunofluorescent staining of histological sections from the testis biopsy of the patient carrying the *SYCE1* variant using γH2AX (Green), H3S10p (red), and DAPI (blue). Scale bar represents 5µm. Early meiotic cells (leptotene/zygotene) were identified based on the presence of many γH2AX-positive patches. No pachytene nuclei with XY bodies could be identified. Instead many spermatocyte nuclei displayed intense γH2AX signal covering the DAPI (DNA) signal, indicating apoptosis. Few, non-apoptotic mitotic metaphases were observed.

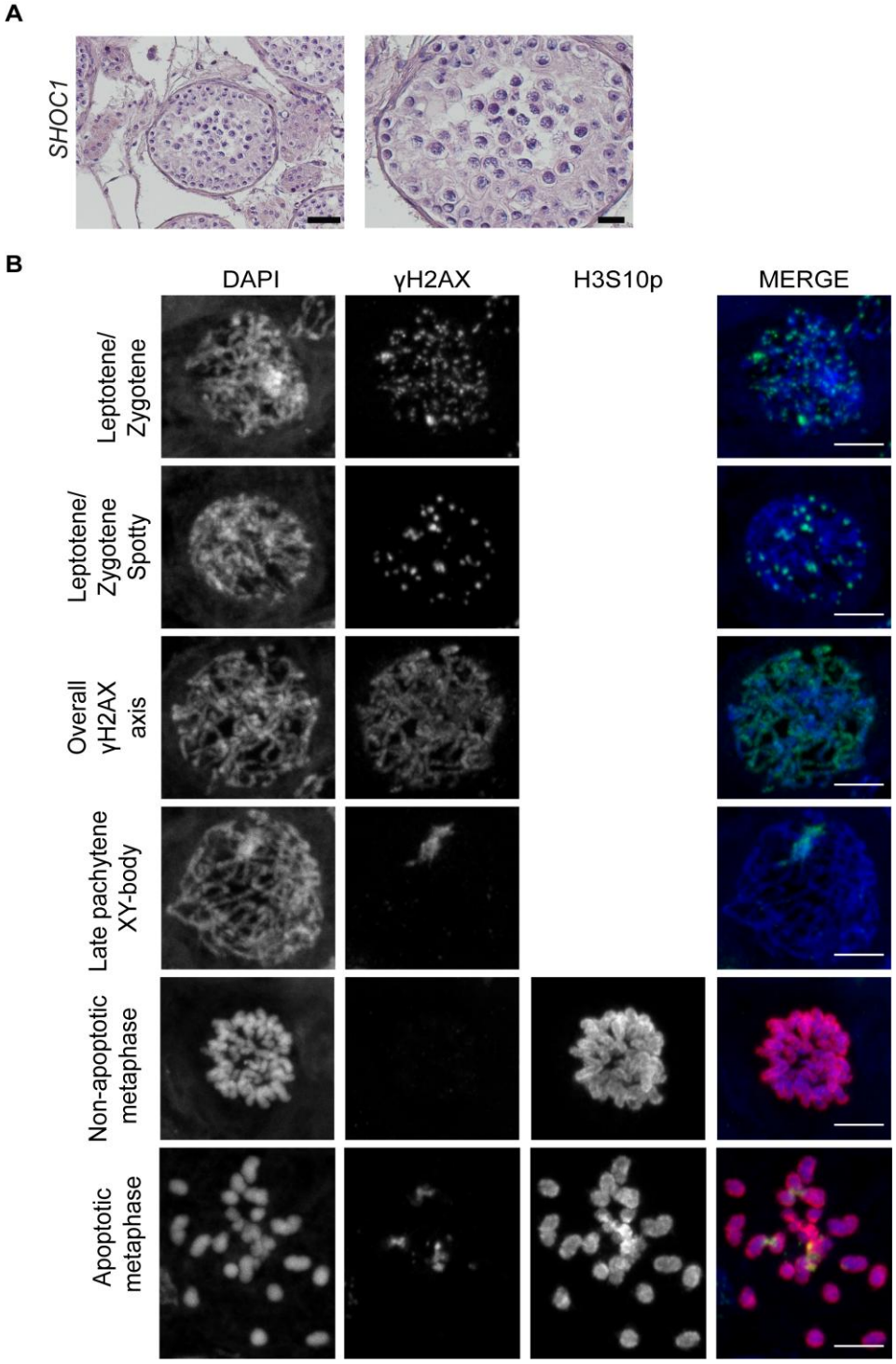

Figure S5. Meiotic progression analysis in patient 11-272 carrying the *SHOC1* variant. A) H&E staining of histological sections from the testis biopsy of the patient carrying the *SHOC1* variant. Scale bar on the left represents 50 µm and on the right, 20 µm. **B)** Immunofluorescent staining of histological sections from the testis biopsy of the patient carrying the *SHOC1* variant using γH2AX (Green), H3S10p (red), and DAPI (blue). Scale bar represents 5µm. Early meiotic cells (leptotene/zygotene) were identified based on the presence of many γH2AX-positive patches. Some spermatocyte nuclei displayed aberrant, intense γH2AX signals ("spotty", "overall γH2AX"). Very rarely, pachytene nuclei with XY bodies were detected. Many meiotic metaphases (identified by H3S10ph), also displayed intense γH2AX signal, indicating apoptosis, and the chromosomes were then often organized in a dispersed pattern.

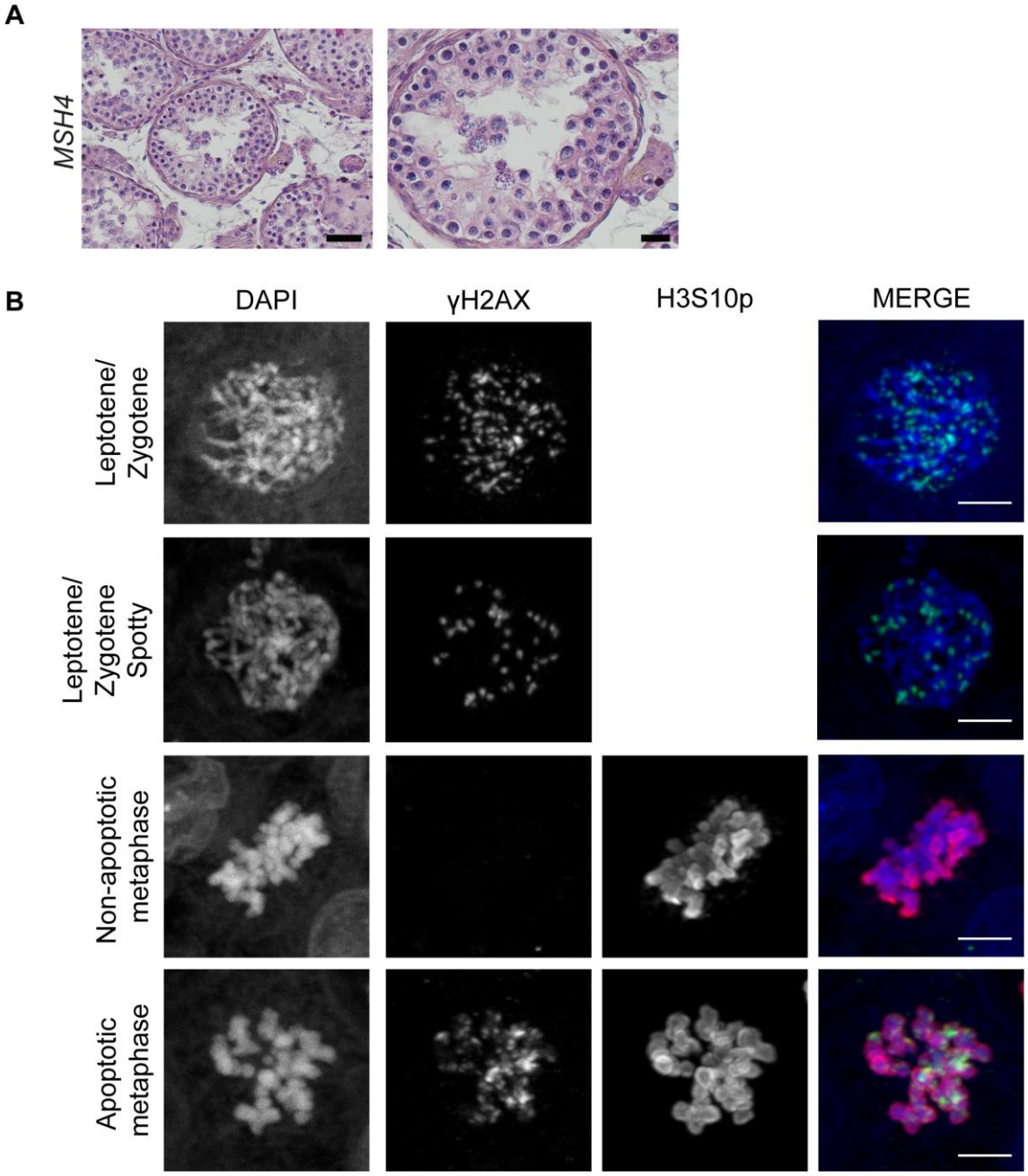

Figure S6. Meiotic progression analysis in patient 11-127 carrying the *MSH4* variant. A) H&E staining of histological sections from the testis biopsy of the patient carrying the *MSH4* variant. Scale bar on the left represents 50 µm and on the right, 20 µm. **B)** Immunofluorescent staining of histological sections from the testis biopsy of the patient carrying the *MSH4* variant using γH2AX (Green), H3S10p (red), and DAPI (blue). Scale bar represents 5µm. Early meiotic cells (leptotene/zygotene) were identified based on the presence of many γH2AX-positive patches. Some spermatocyte nuclei displayed aberrant, intense γH2AX signals ("spotty"). No pachytene nuclei with XY bodies were detected. Many meiotic metaphases (identified by H3S10ph), also displayed intense γH2AX signal, indicating apoptosis.

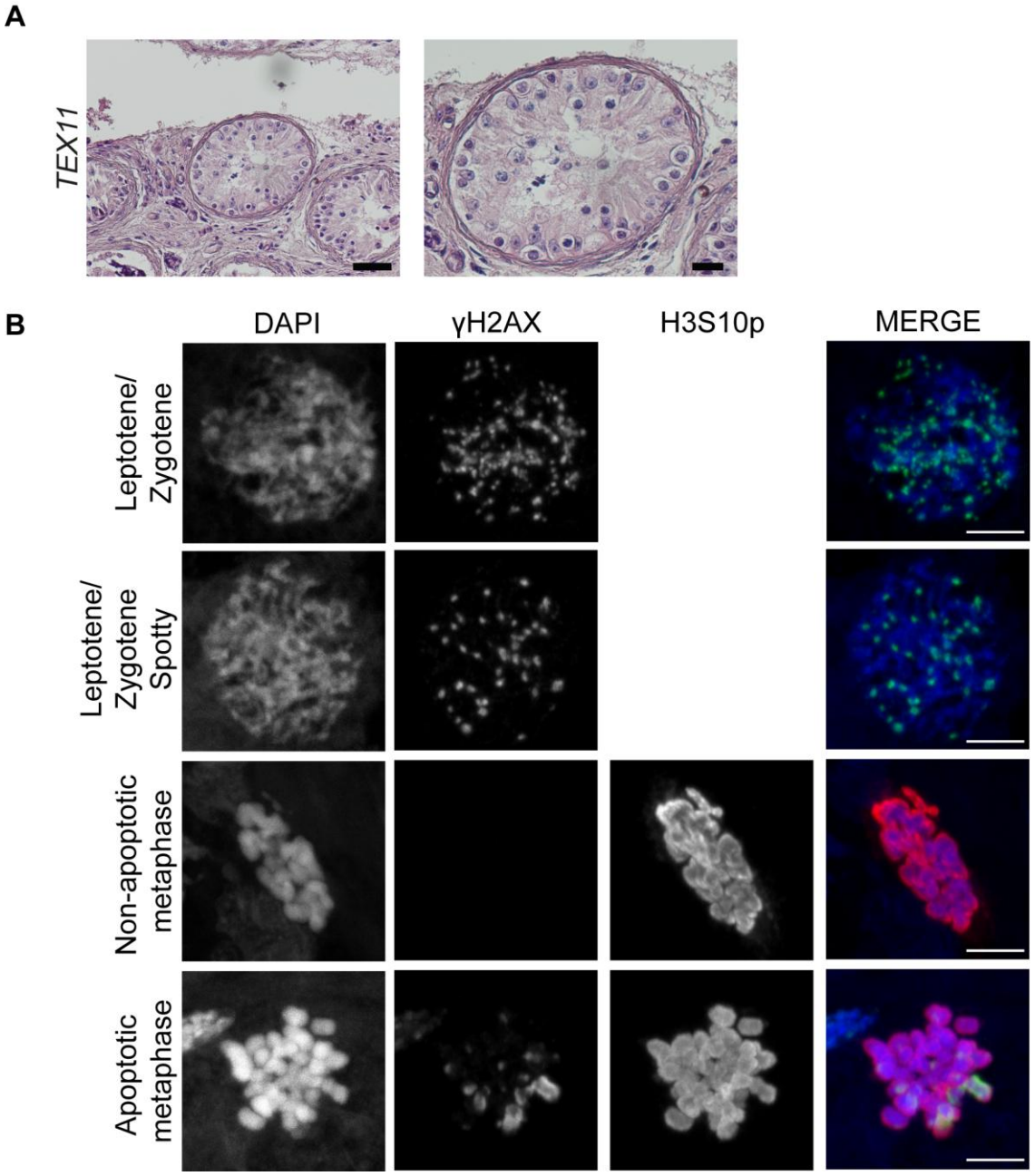

Figure S7. Meiotic progression analysis in patient 09-297 carrying the *TEX11* variant. A) H&E staining of histological sections from the testis biopsy of the patient carrying the *TEX11* variant. Scale bar on the left represents 50 µm and on the right, 20 µm. **B)** Immunofluorescent staining of histological sections from the testis biopsy of the patient carrying the *TEX11* variant using γH2AX (Green), H3S10p (red), and DAPI (blue). Scale bar represents 5µm. Early meiotic cells (leptotene/zygotene) were identified based on the presence of many γH2AX-positive patches. Some spermatocyte nuclei displayed aberrant, intense γH2AX signals ("spotty"). No pachytene nuclei with XY bodies were detected. Many meiotic metaphases (identified by H3S10ph), also displayed intense γH2AX signal, indicating apoptosis.

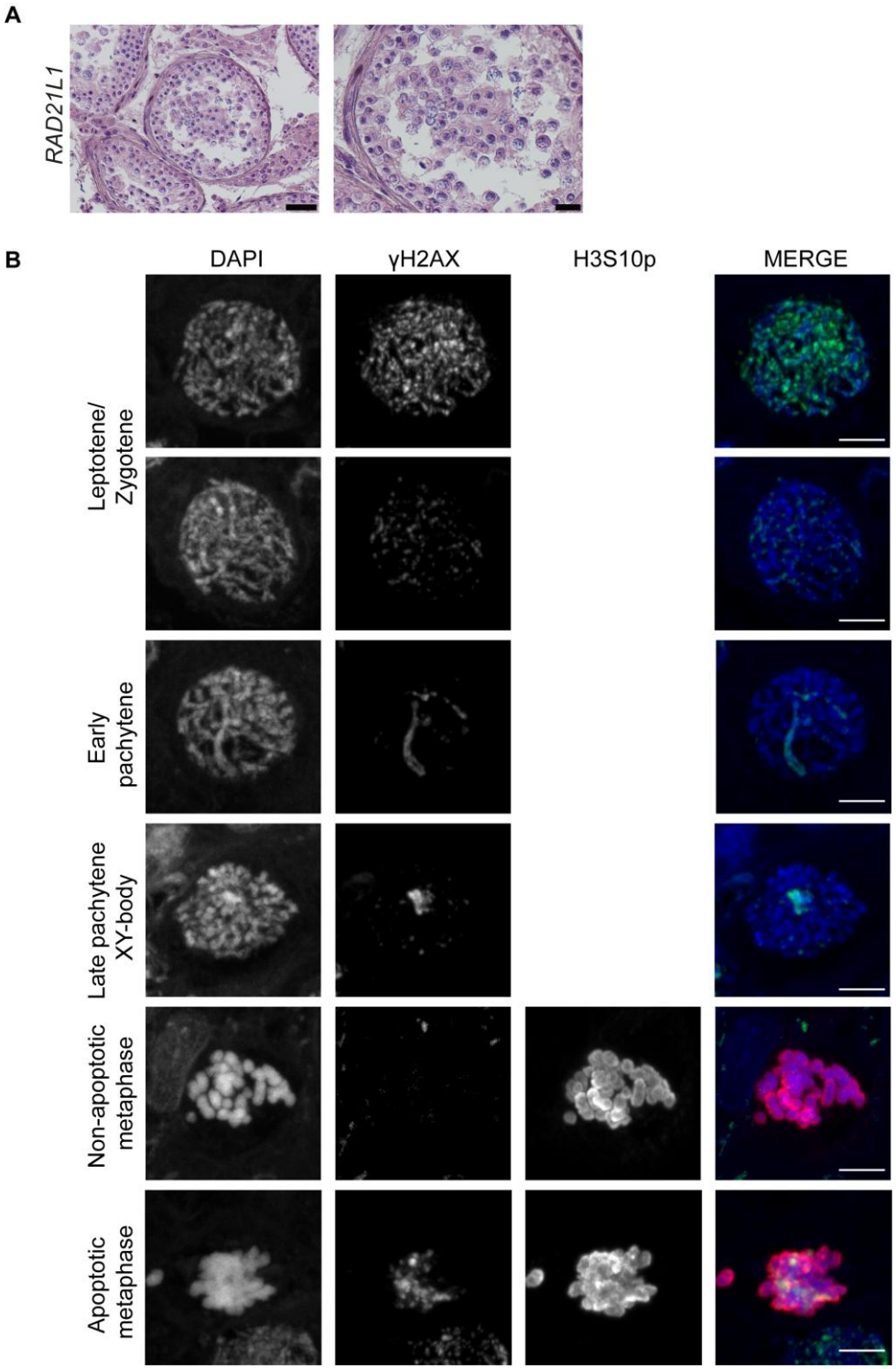

Figure S8. Meiotic progression analysis in patient 07-359 carrying the *RAD21L1* variant. A) H&E staining of histological sections from the testis biopsy of the patient carrying the *RAD21L1* variant. Scale bar on the left represents 50 µm and on the right, 20 µm. **B)** Immunofluorescent staining of histological sections from the testis biopsy of the patient carrying the *RAD21L1* variant using γH2AX (Green), H3S10p (red), and DAPI (blue). Scale bar represents 5µm. The γH2AX patterns indicated normal progression of meiotic prophase up to pachytene. Many meiotic metaphases (identified by H3S10ph), displayed intense γH2AX signal, indicating apoptosis.

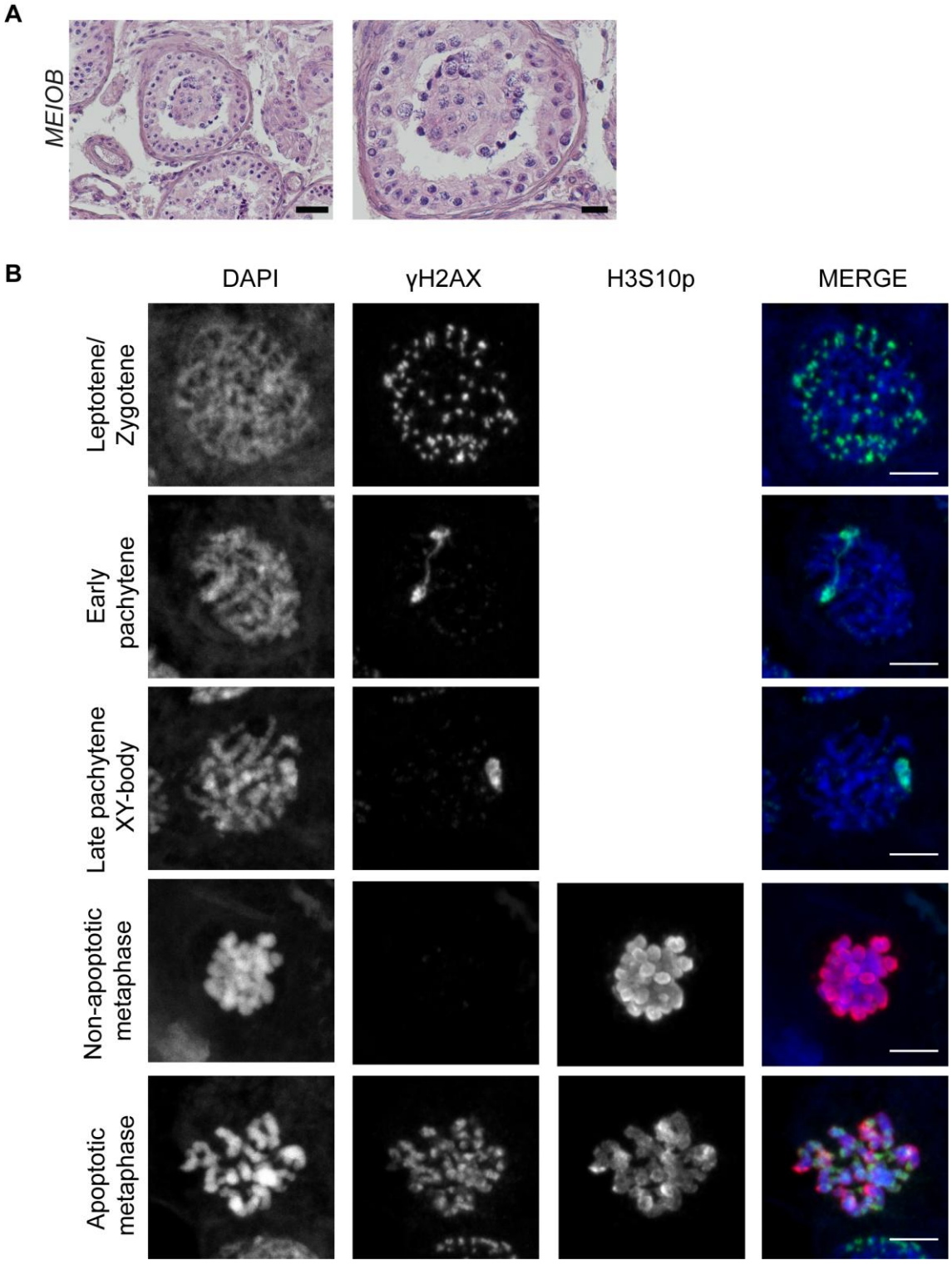

Figure S9. Meiotic progression analysis in patient 08-079 carrying the *MEIOB* variant. A) H&E staining of histological sections from the testis biopsy of the patient carrying the *MEIOB* variant. Scale bar on the left represents 50 µm and on the right, 20 µm. **B)** Immunofluorescent staining of histological sections from the testis biopsy of the patient carrying the *MEIOB* variant using γH2AX (Green), H3S10p (red), and DAPI (blue). Scale bar represents 5µm. The γH2AX patterns indicated normal progression of meiotic prophase up to pachytene. Many meiotic metaphases (identified by H3S10ph), displayed intense γH2AX signal, indicating apoptosis.

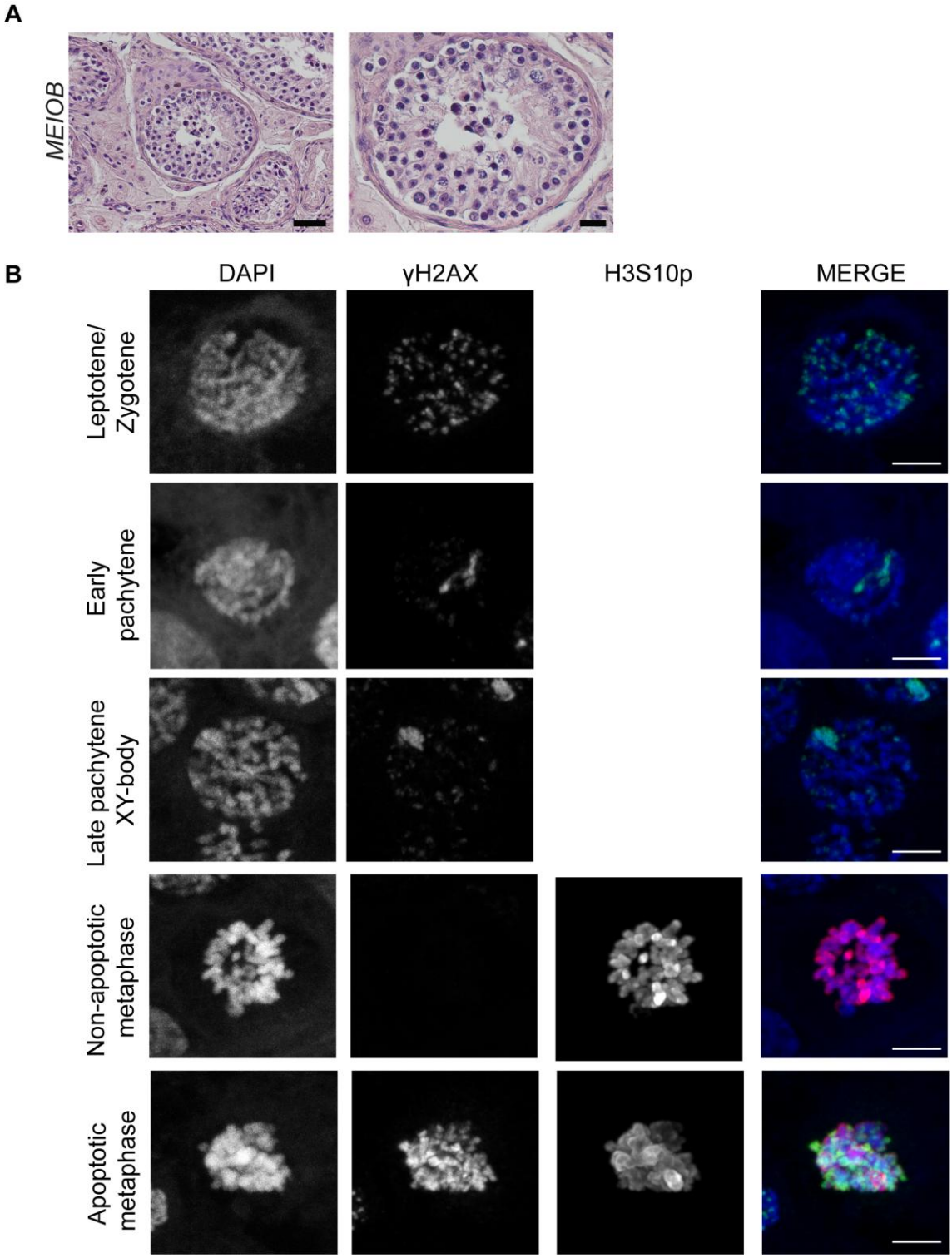

Figure S10. Meiotic progression analysis in patient 09-167 carrying the *MEIOB* variant. A) H&E staining of histological sections from the testis biopsy of the patient carrying the *MEIOB* variant. Scale bar on the left represents 50 µm and on the right, 20 µm. **B)** Immunofluorescent staining of histological sections from the testis biopsy of the patient carrying the *MEIOB* variant using γH2AX (Green), H3S10p (red), and DAPI (blue). Scale bar represents 5µm. The γH2AX patterns indicated normal progression of meiotic prophase up to pachytene. Many meiotic metaphases (identified by H3S10ph), displayed intense γH2AX signal, indicating apoptosis.

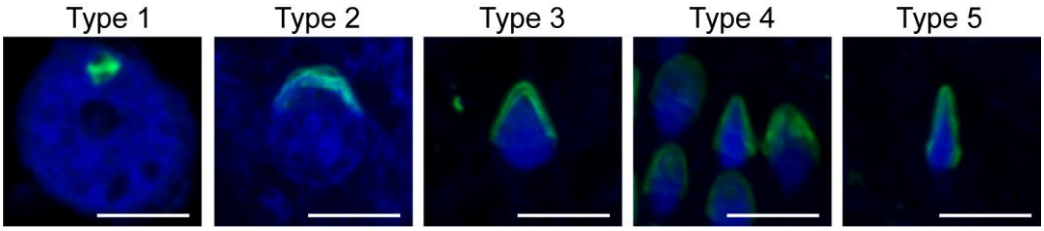

Figure S11. Assessment of elongating spermatids in histological testis tissue sections. Immunofluorescent staining of histological sections from the testis biopsy of a control patient using anti-acrosin (Green) and DAPI (blue). Spermatids are classified according to the developmental stage of the acrosome. Scale bar represents 5µm.

Table S1. Clinical description of the 17 selected NOA patients analyzed by WES and two NOA brothers screened for the variants encountered in the index case

Patient code	Origin	Testicular phenotype	FSH (ref value 1.5-8 IU/L)	Right/Left Testicular volume (mL)
16-231	Spain	Incomplete SCA sp-	5.3	15/15
15-679	Morocco	Incomplete SCA sp-	21	10/12
07-359*	Pakistan	Complete SCA sp-	5.0	14/15
08-079	Spain	Complete SCA sp-	3.7	22/22
09-167	Pakistan	Complete SCA sp-	6.3	18/15
15-285	Venezuela	Complete SCA sp-	4.1	18/15
18-406	Spain	Complete SCA sp-	5.9	20/20
11-127	Morocco	Complete SCA sp-	7.6	15/15
10-200	Spain	Complete SCA sp-	6.1	20/20
10-200 brother	Spain	n.a	8.0	15/15
11-272	Morocco	Complete SCA sp-	8.2	15/13
11-272 brother	Morocco	Complete SCA sp-	11.0	15/12
09-297	India	Complete SCA sp-	4.3	20/20
13-567	Spain	Complete SCA sp-	7.1	18/18
11-151*	Spain	Incomplete SGA sp-	11.0	15/15
17-204	Spain	Incomplete SGA sp-	25.6	12/12
11-063	Morocco	Incomplete SGA sp-	6.4	13/14
17-657	Spain	Incomplete SGA sp-	20.5	11/10
11-382	Spain	Incomplete SGA sp-	11.7	18/15

SCA: SpermatoCytic Arrest; SGA: SpermatogGonial Arrest. *Fertile brother with heterozygous variant, sp-: no sperm retrieved after testicular biopsy; n.a.: no available

Table S3. Quantification of meiotic parameters to assess the type of meiotic arrest

Patient code	**Gene mutated**	**Meiotic entry (%)[a]** (100-43.9)[g]	**XY+T (%)[b]** (100-82.6)[g]	**Mean XY body/XY+T[c]** (32.6-7.74)[g]	**met/mm^2 [d]** (12.54-2.53)[g]	**Apoptotic met (%)[e]** (0-11.5)[g]	**Phenotype[f]**
07-359	*RAD21L1*	100.0%	85.7%	4.0	9.4	53.3%	Complete metaphase arrest
10-200	*TERB1*	81.1%	0.0%	0.0	1.1	7.6%	Failure to form XY body (pachytene arrest)
09-167	*MEIOB*	100.0%	43.4%	1.6	15.3	78.7%	Complete metaphase arrest
11-127	*MSH4*	100.0%	0.0%	0.0	15.2	60.8%	Failure to form XY body/Complete metaphase arrest
15-285	*SYCE1*	100.0%	0.0%	0.0	5.0[g]	1.5%	Failure to form XY body (pachytene arrest)
08-079	*MEIOB*	100.0%	23.5%	1.6	5.1	42.8%	Complete metaphase arrest
11-272	*SHOC1*	95.8%	4.2%	1.0	29.0	84.8%	Extreme reduced XY body formation/Complete metaphase arrest
09-297	*TEX11*	77.2%	0.0%	0.0	12.6	76.0%	Failure to form XY body/Complete metaphase arrest

a) % of tubule sections with early meiotic cells; b) % of XY body-positive tubule sections; c) mean number of nuclei that contain an XY body per XY body-positive tubule section; d) the number of metaphase cells per mm^2 of the section; e) % of metaphases that are apoptotic; f) none of the patients scored positive for spermatids; g) normal range; h) Even though the metaphase density was in the (very low) normal range, the absence of increased metaphase apoptosis, lack of spermatids, complete failure to form the XY body, and apoptotic appearance of spermatocytes with aberrant γH2AX localization pattern indicate pachytene arrest. Red values are outside the normal range established in controls.

Table S4. Comparison of the frequency distribution of subjects with homozygous Loss of Function variants in genes between cases (NOA patients) and controls (subjects in gnomAD v2.1.1_exomes). Fisher's exact test was applied.

Gene	NOA patients (n=147)		Controls in GnomAD (n=125.748)		*p-value*
	Mutated	WT	Mutated	WT	
ADAD2	2	145	1	125.747	0.00000406
RAD21L1	1	146	1	125.747	0.00233393
SHOC1	2	145	0	125.748	0.00000135
SHOC1	3*	144	0	125.748	0.00000000

*Considering the 2 brothers as independent carriers

Table S5. List of variants identified in the five novel candidate genes and their PopScore

Subject	Gene	Variant	PopScore
11-151	*ADAD2*	NM_139174.3:c.1186C>T	n.a
GEMINI-1020	*ADAD2*	NM_001145400.2:c.82dupC	0,000326841
07-359	*RAD21L1*	NM_001136566.2:c.1543C>T	0,000000216
11-272	*SHOC1*	NM_173521.4:c.797delT	0,000026785
M2012	*SHOC1*	NM_173521.4:c.1085_1086delAG	0,000024004
M2046	*SHOC1*	NM_173521.4: c.945_948del	0.000254119
M2046	*SHOC1*	NM_173521.4: c.1351del	0.000254119
M2046	*SHOC1*	NM_173521.4: c.1347T>A	0.000254119
11-127	*MSH4*	NM_002440.4:c.1913C>T	0.000003118
M1916	*MSH4*	NM_002440.4:c.2261C>T	0,000015491
10-200	*TERB1*	NM_001136505.2:c.289_290del	0.000006809
10-200	*TERB1*	NM_001136505.2:c.1813C>T	0,000039868
M468	*TERB1*	NM_001136505.2:c.236C>T	0,000003126

Table S6. Summary of previously reported genes associated with NOA and validated in our study. Genes are ordered according to their updated clinical evidence.

Gene	Number of cases	Testicular phenotype	Type of variant	Status	Reference	Previous clinical evidence (score)	Current clinical evidence (score)
TEX11	2 unrelated NOA cases	SCA, MTA	Partial gene deletion (exons 10,11,12)	hem	Yatsenko et al. 2015[4]	Strong (15)	Definitive (16)
	2 unrelated NOA cases	SCA,	Splice	hem	Yatsenko et al. 2015[4]		
	1 unrelated NOA case	SCA	Missense	hem	Yang et al. 2015[5]		
	1 unrelated NOA case	n.a	Splice	hem	Yang et al. 2015[5]		
	1 unrelated NOA case	SCA	Frameshift insertion	hem	Yang et al. 2015[5]		
	2 brothers	SCA	Missense	hem	Sha et al. 2018[6]		
	1 unrelated NOA case	n.a	Missense	hem	Tüttelmann et al. 2018[7]		
	1 unrelated NOA case	**SCA**	**Partial gene deletion (exons 4,5,6,7,8,9)**	**hem**	**current study**		
TEX14	2 brothers	SCA	Frameshift deletion	hom	Gershoni et al 2017[8]	Limited (7)	Strong (13)
	2 brothers	SCA	Missense	hom	Fahkro et al. 2018[9]		
	1 unrelated NOA case	SCOS	Splice	hom	Fahkro et al. 2018[9]		
	1 unrelated NOA case	SCOS	Frameshift deletion	hom	Fahkro et al. 2018[9]		
	1 unrelated NOA case	MA	Missense+ Missense	het+ het	Fenz Araujo et al. 2019[10]		
	1 unrelated NOA case	**incomplete SGA**	**Frameshift deletion + partial gene deletion**	**hom**	**current study**		
	1 unrelated NOA case	**incomplete SGA**	**Stopgain**	**hom**	**current study**		
STAG3	1 unrelated NOA case	SCA	Frameshift insertion + splicing	het + het	Riera-Escamilla et al. 2019[1]	Moderate $(12)_a$	Strong (13)
	1 unrelated NOA case	SCA	Missense + Missense	het + het	van der Bijl et al. 2019[11]		
	1 unrelated NOA case	**SCA**	**Frameshift deletion + splicing**	**het + het**	**Current study**		
MEIOB	4 brothers	n.a, SCA	Missense	hom	Gershoni et al 2017[8]	Limited (4)	Moderate (11)
	2 brothers	SCA	Frameshift deletion	hom	Gershoni et al 2019[12]		
	1 unrelated NOA case	SCA	Frameshift deletion	hom	Gershoni et al 2019[12]		
	1 unrelated NOA case	**SCA**	**Frameshift deletion**	**hom**	**current study**		
	1 unrelated NOA case	**SCA**	**Partial gene deletion (exons 11,12,13,14)**	**hom**	**current study**		
DMRT1	2 unrelated NOA cases	SCOS, MA	Partial gene deletion: exons 3, 4, 5	het	Lopes et al. 2012[13]	Moderate (9)	Moderate (11)
	1 unrelated NOA case	n.a	Partial gene deletion: exons 3,4	het	Lopes et al. 2012[13]		
	2 unrelated NOA cases	n.a	Complete gene deletion	het	Lopes et al. 2012[13]		
	1 unrelated NOA case	SCA	Missense	het	Tewes et al. 2014[14]		
	1 unrelated NOA case	**incomplete SGA**	**Partial gene deletion: exons 1,2**	**het**	**current study**		
MEI1	2 brothers	SCA	Missense	hom	Ben Khelifa et al. 2018[15]	Limited (5)	Moderate (10)
	1 unrelated NOA case	n.a	Frameshift + splice	het + het	Nguyen et al. 2018[16]		
	1 unrelated NOA case	**SCA**	**Missense**	**het + het**	**current study**		
SYCE1	3 unrelated NOA cases	n.a	Complete gene deletion	hom	Huang et al. 2015[17]	Limited (6)	Not $applicable_b$
	2 brothers	SCA	Splice	hom	Maor-Sagie et al. 2015[18]		
	1 unrelated NOA case	**SCA**	**Complete gene deletion**	**hom**	**current study**		

NOA: Non Obstructive Azoospermia; SCOS: Sertoli Cell Only Syndrome, SGA: SpermatoGonial Arrest; SCA: SpermatoCytic arrest; MA: maturation arrest of unknown stage; MTA; Mixed Testicular Atrophy; n.a: not available; hom: homozygous; het: heterozygous; hem: hemizygous. a: Not included in Oud et al. 2019 because published subsequently. Scoring based on assessment by ARE and CF. b: Assessment of SYCE1 new evidence/score is not applicable because the deletion removes more than one gene

Table S7. Comparison of mouse and human meiotic phenotypes

Gene[refs]	Protein function	Mouse KO phenotype	Male mouse KO arrest	Patient protein variant(s)	Patient phenotype	Patient meiotic arrest type
TERB1[19,20]	Telomere-associated protein, functioning in MAJIN-TERB1-TERB2 complex	Abolishes meiotic chromosomal movement and impairs homologous pairing and synapsis, no XY body formation in males, most advanced stage in males and females is zygotene-like	Pachytene arrest	Compound heterozygote of 103 and 605 aa N-terminal fragment. (homozygous missense variant in highly conserved aa in validation set (MERGE-M468))	Aberrant gH2AX patterns in spermatocytes, no XY bodies, no meiotic metaphases	Pachytene arrest (failure to form the XY body)
SYCE1[21,22]	Structural component of the central element of the synaptonemal complex	Severely impaired synapsis and meiotic DSB repair in both males and females, progression of meiosis up to zygotene-like stage in both males and females. No XY body formation in males	Pachytene arrest	Complete deletion	Aberrant gH2AX patterns in spermatocytes, no XY bodies	Pachytene arrest (failure to form the XY body)
MSH4[23–25]	Member of the DNA mismatch repair mutS family forms the MutS□ complex with MSH5. This complex specifically recognizes Holliday Junctions, which are DSB repair intermediates that usually mature into crossovers.	Severely impaired synapsis and meiotic DSB repair in both males and females, progression of meiosis up to zygotene-like stage in both males and females. No XY body formation in males	Pachytene arrest	Homozygous missense variant in ATPase domain (also homozygous missense variant at different position but also in ATPase domain in validation set (MERGE-M1916)	***Failure to form the XY body, aberrant gH2AX pattern in spermatocytes, apoptotic meiotic metaphases,***	Metaphase arrest
TEX11[26,27]	Homolog of yeast ZIP4, regulator of crossing-over during meiosis. Forms a complex with SHOC1, interacts with MRN complex	Male limited infertility associated with mild repair and synapsis defects and reduced crossover numbers. Cells develop up to metaphase I. Reduced litter size in females	Metaphase arrest	750 aa N-terminal fragment (C-terminal 190aa deleted)	***Failure to form the XY body, aberrant gH2AX pattern in spermatocytes, apoptotic meiotic metaphases,***	Metaphase arrest
SHOC1[28–30]	XPF/MUS81 family member and ATPase required for the formation of crossovers during meiosis. The protein preferentially binds to single-stranded DNA and DNA branches, but it lacks in vitro endonuclease activity. Forms a complex with TEX11 and SPO16	Knockout males and females infertile. Defects in synapsis and DSB repair in males, failure to form the XY body, developmental arrest in zygotene-like stage.	Pachytene arrest	271 aa N-terminal fragment	***Extreme reduction in XY body formation, aberrant gH2AX pattern in spermatocytes, apoptotic meiotic metaphases, with lagging chromosomes***	Metaphase arrest

RAD21L1[31,32]	Component of a meiosis specific component cohesion complex not involved in maintenance of sister chromatid cohesion, but required for homology recognition and completion of meiotic DSB repair	Defects in synapsis and DSB repair in males, failure to form the XY body, developmental arrest in zygotene-like stage. In females only mild defects in synapsis and subfertility due to a POI-like phenotype	Pachytene arrest	Loss of the C-terminal 41 aa, containing a conserved domain	Reduced XY body formation, apoptotic meiotic metaphases	Metaphase arrest
MEIOB[33,34]	Single-stranded DNA-binding protein, meiosis-specific paralog of RPA1, involved in homologous recombination repair	Severely impaired synapsis and meiotic DSB repair in both males and females, progression of meiosis up to zygotene-like stage in both males and females. No XY body formation in males	Pachytene arrest	293 aa, and 381 aa N-terminal fragments in two independent patients	Reduced XY body formation, apoptotic meiotic metaphases	Metaphase arrest
MEI1[35]	Required for meiotic DSB formation	No homologous chromosome pairing or crossover formation due to lack if meiotic DSB formation zygotene-like stage in both males and females. No XY body formation in males	Pachytene arrest	Compound heterozygote of two missense variants in conserved residues	n.a.	SCA
STAG3[36,37]	Meiosis-specific component of the cohesin complex	Male and female infertility, aberrant chromosomal axes, no homologous synapsis, impaired sister chromatid cohesion, no XY body formation in males	Pachytene arrest	Compound heterozygote of splicing variant and frameshift deletion generating 558 aa N-terminal fragment	n.a.	SCA

.

Table S8. Algorithms employed to calculate the index of pathogenicity for variant prioritization in the initial cohort.

Algorithm	Prediction	Meaning	Numeric value (u)
SIFT	T	tolerated	0
	D	damaging	1
Polyphen2_HDIV	B	Benign	0
	P	probably damaging	0.5
	D	damaging	1
Polyphen2_HVAR	B	Benign	0
	P	probably damaging	0.5
	D	damaging	1
Mutation Assessor	N	neutral	0
	L	low	0.25
	M	medium	0.5
	H	high	1
MutationTaster	P	polymorphism	0
	D	damaging	1

Index of pathogenicity (IP) was calculated according to the following formula:

$$\frac{\left(\sum_{r=1}^{n} u_r\right)}{k}$$

Where **k**= number of available prediction tools.

Table S9. Primers employed for variant validation and screening of relatives through Sanger Sequencing (SS), plus/minus PCR, quantitative PCR (qPCR) or Long-Range PCR (LRPCR).

Variant	FW primer (5'-3')	Rev primer (5'-3')	Approach
ADAD2:NM_139174.3:c.1186C>T	TGGCTGGCTGGAGTTCTC	TGTAGAGGTGCAGGAAGACG	SS
ADAD2: NM_001145400.2:c.82dupC + gene deletion	CCATGGCTTCGGCTTCTCA	AGGCACTTTGGGCCTGG	qPCR + SS
chr16:84012049-84224913del (ADAD2 deletion)	TCACCCCACCTCTCATCTCC	AATTTGCCCACCAGTGGCTT	qPCR
DMRT1:NM_021951.3:c.1_540del	TGAAAACAAATGCCCGAAGGT	TTCATGACTGCACTCGCCAT	qPCR
	TCTCTCTCACCTCACTTCGCA	GAGCTGCTCGAGAGGGAAAC	qPCR
MEI1:NM_152513.4:c.925C>T	GAGGCACCTAGGCCAGTTTT	TGTCACCACCCCATCCTTC	SS
MEI1:NM_152513.4:c.1088C>T	TTCTTCCAGTGAAGTGCTCG	GCGAACAGCAGAACATTTGGAT	SS
MEIOB:NM_001163560.3:c.1140_1143del	TTTGCTATTTACCGTGCAGCC	AGTTTTCCACACACTGTCGTA	SS
MEIOB: NM_001163560.3:c.897_1431del	TGCCATAGGAAGGATCAGCTTT	GCTTTCCATTCGGATGTAACCTT	+/- PCR
	CTCCTGAGTCCTAGCCACCA	CATCCGCAGTCCCTTCATAG	+/- PCR
	TCTTCTCCTTGGGCACGAAC	CTCCTGAGTCCTAGCCACCA	+/- PCR
MSH4:NM_002440.4:c.1913C>T	AATTTGGGTGGGGATTTGGGATA	GGCCATAATCTGACAAAGAGCA	SS
MSH4:NM_002440.4:c.2261C>T	TGCTCAGCAGGATGTCTCTA	AAGCTATTTGTGGGTGTCCA	SS
RAD21L1: NM_001136566.2:c.1543C>T	GCCGGCTTTACTTCTAATGATCT	CTGCATAGGGAGCACTCTGG	SS
SHOC1:NM_173521.4:c.797delT	TTCTTGGGTGCCCTTCTAAA	GACTGATCTTGCCATGTTGC	SS
SHOC1:NM_173521.4:c.1085_1086delAG	GCAGAGCCAGGGCCTATATG	AATTCAAGAGCCCCACAGCC	SS
SHOC1:NM_173521.4: c.945_948del	CCCACATTTCTACTCGTTGTACC	CTTGAATCTGGGGCGGAGG	SS
SHOC1:NM_173521.4: c.1351del + NM_173521.4: c.1347T>A	TGGTCCTGTGCAGTCAAGTT	ACACTCGTTTAGGTGTGGAAGT	SS
SHOC1:NM_173521.4: c.945_948del + NM_173521.4: c.1351del + NM_173521.4: c.1347T>A	AGCCAGAGTGAACCAGAAGAGTGC	TGCAGTCAAGTTCAAAGTGATCGT	LRPCR
STAG3: NC_000007.14:g.100180673del	GGCCTCATAGCTCCTCCTCT	TCATCAATGTGGGAAAACGA	SS
STAG3: NM_012447.4:c.1645_1657del	TTGTACAAGGCAGCAACGG	GAGTATTGCTGACCTACCCAC	SS
STAG3: NC_000007.14:g.100180673del+ NM_012447.4:c.1645_1657del	TCCTCTGCCAGTCTACCCTTTG	CACCCTGTCATCGGCTTGGGT	LRPCR
SYCE1: NM_001143764.3: c.1_1113del	ACTGACAGGAAGAAGCAGCC	TGGCGAGCTGAGAGGAAATG	+/- PCR
	CTCTTGTGTGCTCTGGGCTT	TCCACCCTTGATGAGGGACT	+/- PCR
	TGTCCCATTCATATCTTGGCA	ACCACAGCATCCATGTAGGG	+/- PCR

TERB1:NM_001136505.2:c.289_290del	TGGCTGTTCCAATTGATTAAAGTGT	AACCATCGCCAGTTAGGCAA	SS
TERB1:NM_001136505.2:c.1813C>T	TTGTGACGATCACATTGGTATGG	TACCTCCCTCCCAGCACTTATTT	SS
TERB1:NM_001136505.2:c.236C>T	AGGCAAGGAAAGGAACGGAA	TGCACATCCTACAGGTAATGCA	SS
TEX11:NM_001003811.2:c.84_651del	TGTTGCTATCCTTGTGGGCAA	TGCATGTATGAGACTGTGTCTTGT	+/- PCR
	TTGCCTCTGGTATGTTAGGTGA	AGGATCAAGTTCCTTCATGCTGT	+/- PCR
	GTCAGAGAAGGTTTAAACTGCCA	ACAACTTTGGAGTAGAAACCCAGA	+/- PCR
TEX14:NM_001201457.1:c.(554+1_555-1)_(3378+1_3378-1)del	TGCCTCTTGAACAAGCCAAG	TGAACCCTTGGTGAATGAGG	qPCR
	TTCCTTGCATTTCTGGTTCAG	AGGACAGGGGACTGGAAGAC	qPCR
	AATTTGGGTTGACAAAGATTCAGTA	TGGGCAAAATCTCAGCATTC	qPCR
TEX14:NM_001201457.1:c.3454C>T	GCTAAGCTGCCCAAAGCTAAC	TCTTTCAGGTGAGGAAAAGTTCCA	SS
TEX14:NM_001201457.1:c.2303_2306del	GGTAGGGTTGGGTAGTTGCC	GGACTGGCAAAACGGTTCAC	SS

Table S10. Commercially available TaqMan gene expression assays used in this study for the analysis of RNA derived from testis biopsies.

Gene	**Function**	**Assay ID**
ADAD2	Target gene	Hs00952793_g1
DAZ	Spermatogonia/early spermatocytes biomarker	Hs00414014_m1
BRDT	Pachytene spermatocytes/round and elongating spermatids	Hs00976114_m1
CDY1	Spermatids biomarker	Hs00371514_m1
PRM2	Spermatids/mature spermatozoa biomarker	Hs04187294_g1
GAPDH	Reference housekeeping gene	Hs0275891_g1

SUPPLEMENTARY REFERENCES

1. Riera-Escamilla A, Enguita-Marruedo A, Moreno-Mendoza D, et al. Sequencing of a "mouse azoospermia" gene panel in azoospermic men: identification of RNF212 and STAG3 mutations as novel genetic causes of meiotic arrest. *Hum Reprod*. 2019;34(6):978-988. doi:10.1093/humrep/dez042.

2. Enguita-Marruedo A, Sleddens-Linkels E, Ooms M, et al. Meiotic arrest occurs most frequently at metaphase and is often incomplete in azoospermic men. *Fertil Steril*. November 2019. doi:10.1016/j.fertnstert.2019.08.004.

3. Wilfert AB, Chao KR, Kaushal M, et al. Genome-wide significance testing of variation from single case exomes. *Nat Genet*. 2016;48(12):1455-1461. doi:10.1038/ng.3697.

4. Yatsenko AN, Georgiadis AP, Ropke A, et al. X-linked TEX11 mutations, meiotic arrest, and azoospermia in infertile men. *N Engl J Med*. 2015;372(22):2097-2107. doi:10.1056/NEJMoa1406192.

5. Yang F, Silber S, Leu NA, et al. TEX11 is mutated in infertile men with azoospermia and regulates genome-wide recombination rates in mouse. *EMBO Mol Med*. 2015;7(9):1198-1210. doi:10.15252/emmm.201404967.

6. Sha Y, Zheng L, Ji Z, et al. A novel TEX11 mutation induces azoospermia: a case report of infertile brothers and literature review. *BMC Med Genet*. 2018;19(1):63. doi:10.1186/s12881-018-0570-4.

7. Tuttelmann F, Ruckert C, Ropke A. Disorders of spermatogenesis: Perspectives for novel genetic diagnostics after 20 years of unchanged routine. *Medizinische Genet Mitteilungsblatt des Berufsverbandes Medizinische Genet eV*. 2018;30(1):12-20. doi:10.1007/s11825-018-0181-7.

8. Gershoni M, Hauser R, Yogev L, et al. A familial study of azoospermic men identifies three novel causative mutations in three new human azoospermia genes. *Genet Med*. February 2017. doi:10.1038/gim.2016.225.

9. Fakhro KA, Elbardisi H, Arafa M, et al. Point-of-care whole-exome sequencing of idiopathic male infertility. *Genet Med*. 2018;20(11):1365-1373. doi:10.1038/gim.2018.10.

10. Fenz Araujo T, Friedrich C, Paiva Grangeiro CH, et al. Sequence analysis of 37 candidate genes for male infertility: Challenges in variant assessment and validating genes. *Andrology*. September 2019. doi:10.1111/andr.12704.

11. van der Bijl N, Ropke A, Biswas U, et al. Mutations in the stromal antigen 3 (STAG3) gene cause male infertility due to meiotic arrest. *Hum Reprod*. November 2019. doi:10.1093/humrep/dez204.

12. Gershoni M, Hauser R, Barda S, et al. A new MEIOB mutation is a recurrent cause for azoospermia and testicular meiotic arrest. *Hum Reprod*. 2019;34(4):666-671. doi:10.1093/humrep/dez016.

13. Lopes AM, Aston KI, Thompson E, et al. Human spermatogenic failure purges deleterious mutation load from the autosomes and both sex chromosomes, including the gene DMRT1. *PLoS Genet*. 2013;9(3):e1003349.

doi:10.1371/journal.pgen.1003349.

14. Tewes A-C, Ledig S, Tuttelmann F, Kliesch S, Wieacker P. DMRT1 mutations are rarely associated with male infertility. *Fertil Steril*. 2014;102(3):816-820.e3. doi:10.1016/j.fertnstert.2014.05.022.

15. Ben Khelifa M, Ghieh F, Boudjenah R, et al. A MEI1 homozygous missense mutation associated with meiotic arrest in a consanguineous family. *Hum Reprod*. 2018;33(6):1034-1037. doi:10.1093/humrep/dey073.

16. Nguyen NMP, Ge Z-J, Reddy R, et al. Causative Mutations and Mechanism of Androgenetic Hydatidiform Moles. *Am J Hum Genet*. 2018;103(5):740-751. doi:10.1016/j.ajhg.2018.10.007.

17. Huang N, Wen Y, Guo X, et al. A Screen for Genomic Disorders of Infertility Identifies MAST2 Duplications Associated with Nonobstructive Azoospermia in Humans. *Biol Reprod*. 2015;93(3):61. doi:10.1095/biolreprod.115.131185.

18. Maor-Sagie E, Cinnamon Y, Yaacov B, et al. Deleterious mutation in SYCE1 is associated with non-obstructive azoospermia. *J Assist Reprod Genet*. 2015;32(6):887-891. doi:10.1007/s10815-015-0445-y.

19. Shibuya H, Ishiguro K, Watanabe Y. The TRF1-binding protein TERB1 promotes chromosome movement and telomere rigidity in meiosis. *Nat Cell Biol*. 2014;16(2):145-156. doi:10.1038/ncb2896.

20. Wang Y, Chen Y, Chen J, et al. The meiotic TERB1-TERB2-MAJIN complex tethers telomeres to the nuclear envelope. *Nat Commun*. 2019;10(1):564. doi:10.1038/s41467-019-08437-1.

21. Bolcun-Filas E, Hall E, Speed R, et al. Mutation of the mouse Syce1 gene disrupts synapsis and suggests a link between synaptonemal complex structural components and DNA repair. *PLoS Genet*. 2009;5(2):e1000393. doi:10.1371/journal.pgen.1000393.

22. Hamer G, Gell K, Kouznetsova A, Novak I, Benavente R, Hoog C. Characterization of a novel meiosis-specific protein within the central element of the synaptonemal complex. *J Cell Sci*. 2006;119(Pt 19):4025-4032. doi:10.1242/jcs.03182.

23. Bocker T, Barusevicius A, Snowden T, et al. hMSH5: a human MutS homologue that forms a novel heterodimer with hMSH4 and is expressed during spermatogenesis. *Cancer Res*. 1999;59(4):816-822.

24. Snowden T, Acharya S, Butz C, Berardini M, Fishel R. hMSH4-hMSH5 recognizes Holliday Junctions and forms a meiosis-specific sliding clamp that embraces homologous chromosomes. *Mol Cell*. 2004;15(3):437-451. doi:10.1016/j.molcel.2004.06.040.

25. Kneitz B, Cohen PE, Avdievich E, et al. MutS homolog 4 localization to meiotic chromosomes is required for chromosome pairing during meiosis in male and female mice. *Genes Dev*. 2000;14(9):1085-1097.

26. Adelman CA, Petrini JHJ. ZIP4H (TEX11) deficiency in the mouse impairs meiotic double strand break repair and the regulation of crossing over. *PLoS Genet*. 2008;4(3):e1000042. doi:10.1371/journal.pgen.1000042.

27. Yang F, Gell K, van der Heijden GW, et al. Meiotic failure in male mice lacking an X-linked factor. *Genes Dev*. 2008;22(5):682-691. doi:10.1101/gad.1613608.

28. Guiraldelli MF, Felberg A, Almeida LP, Parikh A, de Castro RO, Pezza RJ. SHOC1 is a ERCC4-(HhH)2-like protein, integral to the formation of crossover recombination intermediates during mammalian meiosis. *PLoS Genet*. 2018;14(5):e1007381. doi:10.1371/journal.pgen.1007381.

29. Zhang Q, Ji S-Y, Busayavalasa K, Yu C. SPO16 binds SHOC1 to promote homologous recombination and crossing-over in meiotic prophase I. *Sci Adv*. 2019;5(1):eaau9780. doi:10.1126/sciadv.aau9780.

30. Zhang Q, Shao J, Fan H-Y, Yu C. Evolutionarily-conserved MZIP2 is essential for crossover formation in mammalian meiosis. *Commun Biol*. 2018;1:147. doi:10.1038/s42003-018-0154-z.

31. Herran Y, Gutierrez-Caballero C, Sanchez-Martin M, et al. The cohesin subunit RAD21L functions in meiotic synapsis and exhibits sexual dimorphism in fertility. *EMBO J*. 2011;30(15):3091-3105. doi:10.1038/emboj.2011.222.

32. Llano E, Herran Y, Garcia-Tunon I, et al. Meiotic cohesin complexes are essential for the formation of the axial element in mice. *J Cell Biol*. 2012;197(7):877-885. doi:10.1083/jcb.201201100.

33. Souquet B, Abby E, Herve R, et al. MEIOB targets single-strand DNA and is necessary for meiotic recombination. *PLoS Genet*. 2013;9(9):e1003784. doi:10.1371/journal.pgen.1003784.

34. Luo M, Yang F, Leu NA, et al. MEIOB exhibits single-stranded DNA-binding and exonuclease activities and is essential for meiotic recombination. *Nat Commun*. 2013;4:2788. doi:10.1038/ncomms3788.

35. Libby BJ, De La Fuente R, O'Brien MJ, et al. The mouse meiotic mutation mei1 disrupts chromosome synapsis with sexually dimorphic consequences for meiotic progression. *Dev Biol*. 2002;242(2):174-187. doi:10.1006/dbio.2001.0535.

36. Hopkins J, Hwang G, Jacob J, et al. Meiosis-specific cohesin component, Stag3 is essential for maintaining centromere chromatid cohesion, and required for DNA repair and synapsis between homologous chromosomes. *PLoS Genet*. 2014;10(7):e1004413. doi:10.1371/journal.pgen.1004413.

37. Winters T, McNicoll F, Jessberger R. Meiotic cohesin STAG3 is required for chromosome axis formation and sister chromatid cohesion. *EMBO J*. 2014;33(11):1256-1270. doi:10.1002/embj.201387330.